RELATIVISTIC EMISSION FEATURES IN THE SPECTRA OF SEYFERT 1 GALAXIES

G. Branduardi-Raymont [a] M. Sako [b] S. M. Kahn [c] J. S. Kaastra [d] K. O. Mason [a] P. M. Ogle [e] M. J. Page [a] E. M. Puchnarewicz [a] N. Salvi [a] K. C. Steenbrugge [d]

[a]MSSL, University College London, Holmbury St. Mary, Dorking, Surrey RH5 6NT, UK

[b]Theoretical Astrophysics and Space Radiation Laboratory, Caltech, MC 130-33, Pasadena, CA 91125, USA

[c]Department of Physics, Columbia University, 550 West 120th Street, New York, NY 10027, USA

[d]SRON, National Institute for Space Research, Sorbonnelaan 2, 3584 CA Utrecht, The Netherlands

[e]Department of Physics, University of California, Santa Barbara, CA 93106, USA

We review the evidence for broad soft X-ray relativistic emission lines in Seyfert 1 galaxies: these spectral features, revealed for the first time by observations with the *XMM-Newton* Reflection Grating Spectrometer in MCG −6-30-15 and Mrk 766, have been detected in a number of other objects, at lower significance. Despite having raised some controversy, their interpretation in terms of emission lines from a relativistic accretion disk around a supermassive Kerr black hole still appears to be the more favourable model, and is reinforced by the recent observation of one strong feature of the same kind in NGC 4051, and by the indication that their presence may be related to that of a broad Fe line at higher energies. Theory shows that the lines can originate in the hot surface layer of an accretion disk in hydrostatic equilibrium and ionised by X-ray illumination, thus providing further support to our interpretation.

1. Introduction

The launch of the *Chandra* and *XMM-Newton* observatories in 1999 has led to a giant step in quality and quantity of data available to X-ray astronomy; in no other context is this more true than high resolution X-ray spectroscopy: its unique diagnostic power can now be deployed on all kind of cosmic X-ray sources, and is no longer limited to solar studies as it has been the case until the end of the last decade.

Just over two years ago (summer 2000) *XMM-Newton* Reflection Grating Spectrometer (RGS) data of two Seyfert 1 galaxies, MCG −6-30-15 and Mrk 766, revealed spectral features with a 'saw-tooth' profile never observed before at soft X-ray energies (<2 keV). Fig. 1 shows the RGS data and the features emerging over the extrapolation of the higher energy continuum measured simultaneously with the *XMM-Newton* EPIC pn camera. The similarity of the two spectra is striking, as they display exactly the same features, peaking at $\sim$ 18, 24 and 33 Å, respectively. In both cases the data cannot be fitted by standard warm absorber models [1]: first, the features are at the wrong wavelengths to be explained as edges imprinted by ionised gas; second, if they were edges, they would be too deep to be associated with the narrow absorption lines also present in the spectra, which imply much lower column densities of absorbing gas. However, a good fit can be achieved if we interpret the features as emission lines of O VIII Lyα (rest frame λ = 18.97 Å), N VII Lyα (24.78 Å) and C VI Lyα (33.73 Å), broadened and distorted by relativistic and gravitational effects in an accretion disk in the vicinity of a spinning supermassive black hole. These features would be the low energy anologue of the broad Fe Kα line at $\sim$ 6 keV discovered by *ASCA* in MCG −6-30-15 [2], and later reported to be present in the *ASCA* spectra of many Seyfert galaxies. Fig. 2 shows the best fits to the RGS data, obtained with a model including a power law continuum and three emission features (characterised by Laor profiles [3]), seen through a warm absorber ([4] gives details of the model and best fit parameters).

The discrete features detected in MCG −6-30-15 and Mrk 766 by the RGS appear even more

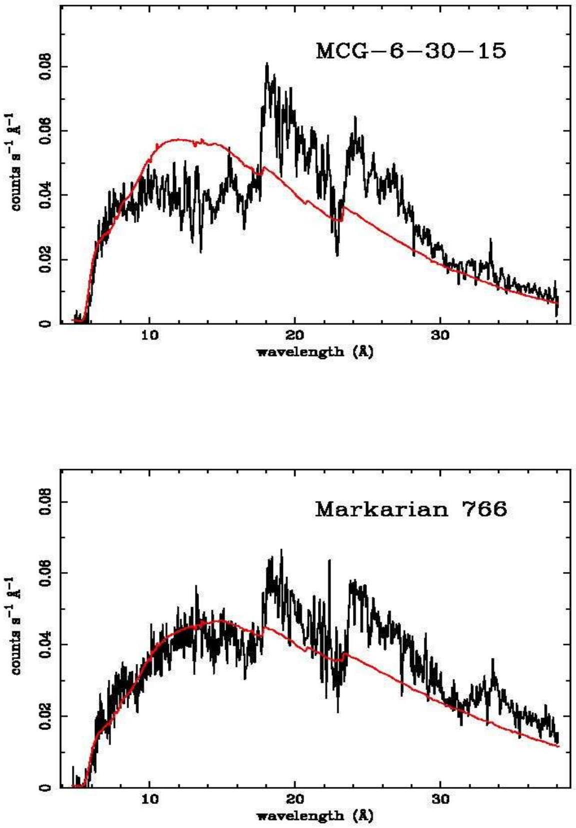

Figure 1. RGS-1 and -2 spectra combined (black) of MCG −6-30-15 (top) and Mrk 766 (bottom) with the best fitting power law continuum from the EPIC pn camera overposed (red).

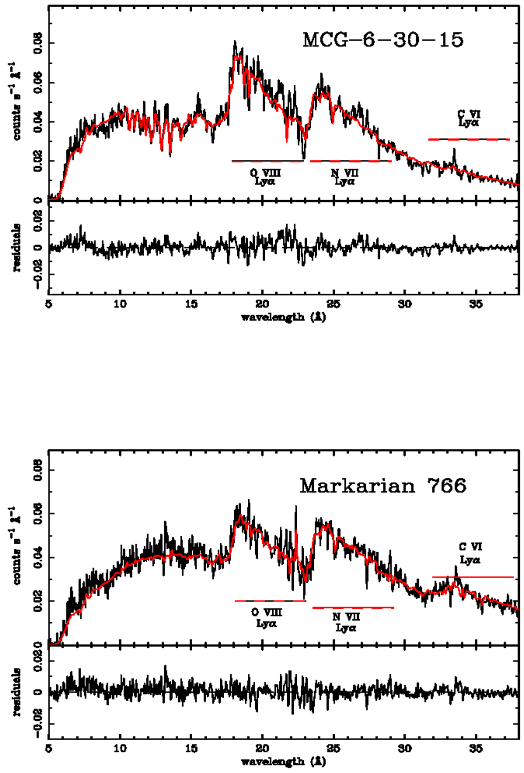

Figure 2. Top and bottom: RGS spectra (black) and best fit models (red) for MCG −6-30-15 and Mrk 766 respectively; the models comprise a power law, Galactic absorption, three relativistic disk emission lines and warm absorption.

remarkable when compared to the RGS spectra of other active galaxies which display no broad emission features, and are dominated by absorption in the ionised gas surrounding the nucleus (e.g. IRAS13349+2438; see Fig. 3, from [5]).

2. The MCG −6-30-15 alternative

The novel idea that relativistic emission features could appear in the soft X-ray spectra of AGN, just as they had been reported at higher energies, was naturally challenged. In particular, a recent *Chandra* HETGS observation of MCG −6-30-15 was taken to indicate that the spectrum of this galaxy is dominated by dusty warm absorption, with no requirement for any emission features [6]. In this case the best fit would comprise a power law continuum and a soft excess modeled as a blackbody, both seen through a warm absorber with dust embedded in it. The main argument of Lee *et al.* is that the sharp 'edge' at $\sim$ 18 Å in MCG −6-30-15 (see Fig. 1) is caused by a combination of O VII and neutral Fe L-shell absorption (with a column density $N_{FeI} \sim 4 \times 10^{17}$ cm^{-2}). To avoid large amounts of neutral absorption to show up elsewhere in the spectrum, the iron has to be locked up in dust grains, presumably in the form of oxides.

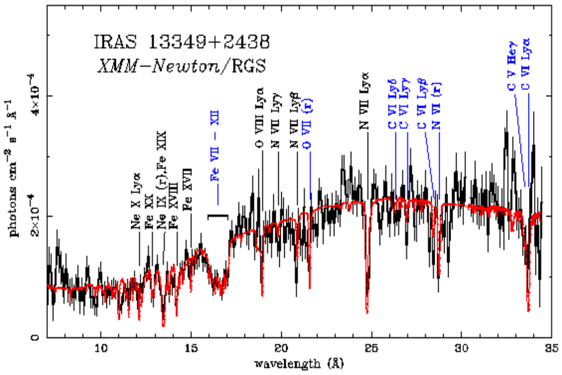

Figure 3. RGS spectrum of IRAS13349+2438, illustrating the case of an active galaxy dominated by absorption in ionised gas surrounding the nucleus.

We decided to carry out a direct test of the Lee *et al.* model on the MCG −6-30-15 RGS data [4]. A first attempt, by fixing the index and normalisation of the power law at the values derived from the EPIC pn spectrum, and the blackbody temperature at the Lee *et al.* value (0.13 keV) results in a reasonable fit in the region below ∼ 23 Å, where HETGS and RGS overlap in bandpass. However, the model is well above the data at longer wavelengths (Fig. 4, top), in the band where HETGS has essentially no response. In particular, the large jump at the neutral oxygen edge at 23 Å (required by the column of dust) is a severe mismatch to the observed spectrum. Letting the blackbody temperature free improves the fit (Fig. 4, bottom): the blackbody is hotter, and less dust is required. However, the details of the data are still not well reproduced; in particular the depth of the O VII narrow absorption lines is overestimated [4].

3. The longer observation of Mrk 766

A second, longer (130 ks vs 56 ks) observation of Mrk 766 in May 2001 confirmed the presence of the peaked and broad features in the RGS spectrum, with many narrow absorption lines superimposed [7]. Again the spectrum is well fitted by three asymmetric emission lines seen through a warm absorber, whose details are much clearer because of the higher signal-to-noise ratio of the

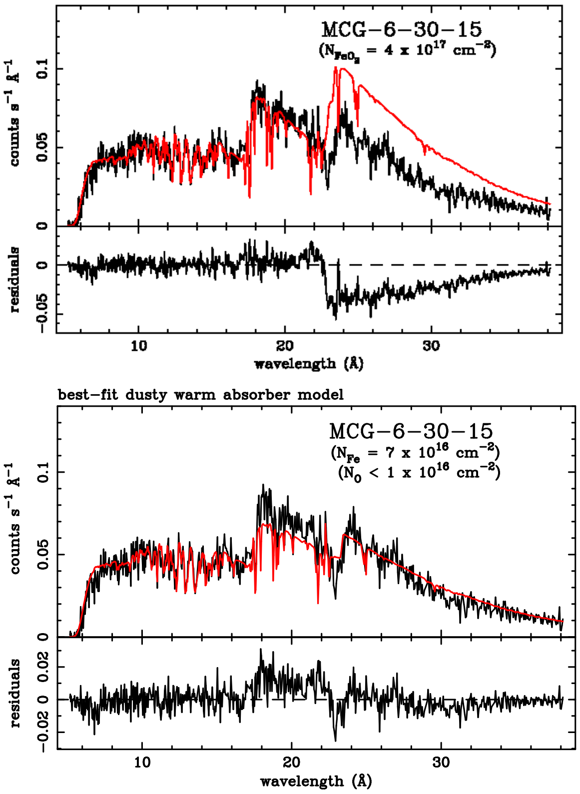

Figure 4. *Top*: The Lee *et al.* model (red) superimposed on the RGS data of MCG −6-30-15 (black). Notice the severe mismatch above ∼ 23 Å; see text for details. *Bottom*: Lee *et al.* model (red) fitted to the RGS data of MCG −6-30-15 (black). Although there is better agreement with the data, the residuals still show systematic deviations.

data (in addition to the longer exposure, the average source flux was 50% brighter than in the first observation).

The 2001 RGS spectrum of Mrk 766 is shown in Fig. 5, together with the model components used in two different spectral fits: DWA includes a two-power-law continuum upon which edges are imprinted by a warm absorber with dust; REL comprises a power law continuum and three relativistic emission lines, all absorbed by warm gas (see [7] for details).

A direct comparison of the two fits is shown in Fig. 6. The DWA fit cannot properly account for the peaked features in the data; in particular,

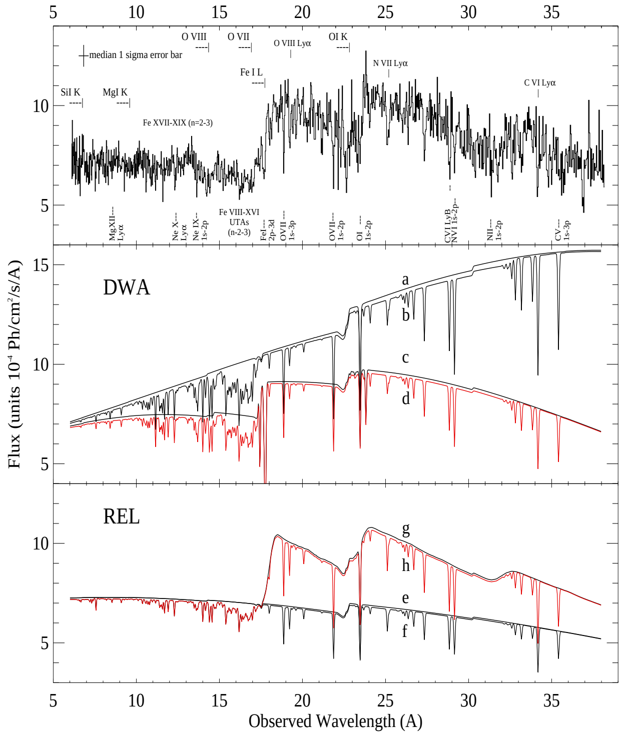

Figure 5. RGS-1 and -2 data combined from the second longer observation of Mrk 766 (top panel); spectral features that may be expected in this band are indicated. DWA and REL model fits (see text) are shown in the middle and lower panels respectively: best fit models, curves d and h, are in red; a and e are the underlying continua, b and f are the continua seen through the warm absorbers, c shows the DWA continuum seen through dust, and g the REL continuum plus relativistic lines.

the residuals show a clear excess longward of 17 Å. The edges could be made deeper by increasing the flux in the soft power law, but the overall spectral shape would then be wrong. Given the fitted depth of the Fe I edge near 17 Å, one would expect a much stronger Fe I absorption line than is observed at $\sim$ 17.7 Å. Visually, the REL model residuals indicate less systematic deviations. The emission line energies are consistent with the Lyα transitions identified in the first observation of Mrk 766. Formally the best fit REL model gives χ^2/d.o.f. = 1.7, significantly better than the DWA model (χ^2/d.o.f. = 2.2), although still rather high. Inner shell resonance lines from low ionisation species, not yet included in the model, may contribute significantly to increasing the χ^2 value.

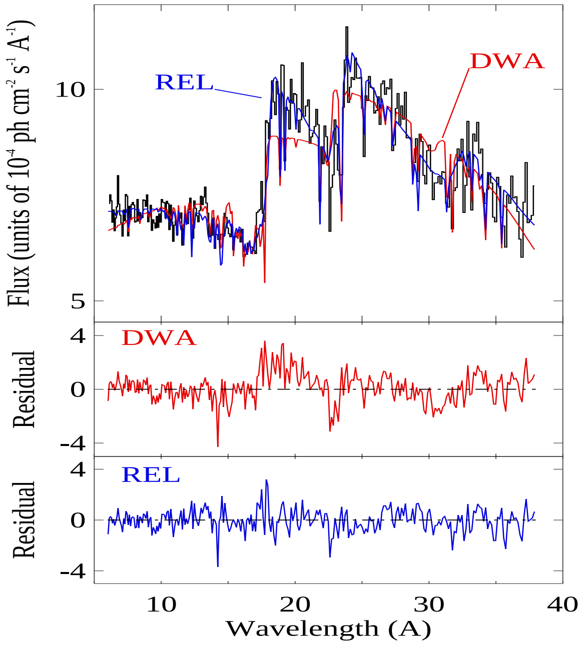

Figure 6. Comparison of the DWA and REL fits to the RGS data from the second observation of Mrk 766; the data are binned by a factor of four for clarity.

The EPIC MOS-2 data obtained simultaneously to the RGS spectra during the 2001 longer observation of Mrk 766 show the presence of an asymmetric, relativistically broadened Fe Kα line whose red wing extends down to about 3 keV. Its best fit energy (6.7 keV) is indicative of highly ionised iron, and its shape (modeled with a Laor profile) is consistent with the parameters derived for the three low energy lines observed with RGS [7]. Fig. 7 shows the Fe line profile scaled to the energy of the O VIII line and superimposed to it. The good agreement between the two strengthens the idea that the RGS spectral features are emission lines from a relativistic disk.

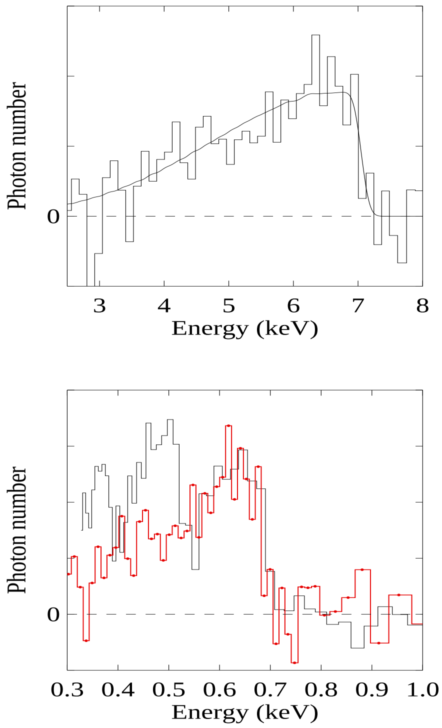

Figure 7. *Top*: Fe Kα line profile of Mrk 766, as observed with EPIC MOS-2 (the histogram shows the residuals above the best fit continuum); the best fit relativistic line model is superimposed as a continuous line. *Bottom*: The red histogram is the Fe Kα line profile from EPIC MOS-2, scaled to the energy of the O VIII line and plotted over it.

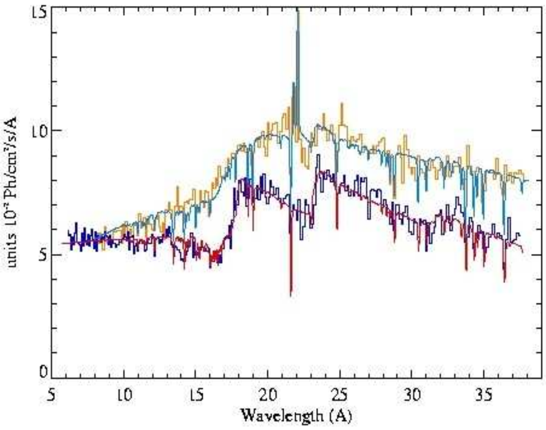

Figure 8. RGS spectrum of NGC 4051 (upper histogram) compared with that of Mrk 766 (lower histogram). The best fit REL models (also including O VII narrow emission lines for NGC 4051) are shown in contrasting colours.

4. NGC 4051

A 103 ks *XMM-Newton* observation of NGC 4051 in May 2001 has provided a high quality RGS spectrum, which is shown and compared with that of Mrk 766 in Fig. 8.

The two spectra have a very different appearance: instead of the three saw-tooth emission features seen in Mrk 766, NGC 4051 displays a broad peak centred at $\sim$ 20 Å. The O VII forbidden emission line is strong in NGC 4051 but very weak in Mrk 766. NGC 4051 shows several narrow absorption lines indicative of a warm absorber but there is no evidence for the broad Fe UTA (Unresolved Transition Array) present in the spectrum of Mrk 766 near 16 Å, nor for any feature that could be interpreted as a neutral Fe L edge due to dust. However, the bump at $\sim$ 20 Å can be modeled with very broad relativistic emission due to O VIII Lyα, Lyβ, plus higher order lines and RRC (Radiative Recombination Continuum). If there is any underlying N VII emission, it must be at a much lower level than in Mrk 766. The exceptional profile in NGC 4051 requires more extreme Laor model parameters than those of Mrk 766: a higher inclination disk ($i \sim 50^o$ rather than $\sim 35^o$), and a larger emissivity index ($q \sim 6$ instead of ~ 3.5). Also in the case of NGC 4051 it is interesting to compare the profile of the Fe Kα line, as measured by EPIC MOS-2 (shown in Fig. 9), with that of the O VIII line observed by RGS (Fig. 8). NGC 4051 shows a strong narrow Fe component at 6.4 keV superimposed on a very broad emission feature whose red wing extends down to about 3 keV, very reminiscent of those in Mrk 766 (Fig. 7) and MCG $-$6-30-15 (see [8]). Again the similarity of this broad profile with that of the soft X-ray O VIII emission line in NGC 4051 suggests that both may have a similar origin in a relativistic accretion disk.

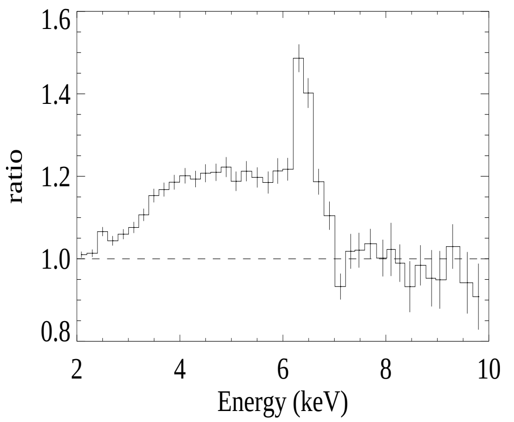

Figure 9. Profile of the Fe Kα emission observed in NGC 4051 with the EPIC MOS-2 camera. The histogram is the ratio of the data to the best fit continuum model.

5. A plausible physical model

As discussed in [4], the emission features detected in the soft X-ray RGS spectra of MCG −6-30-15 and Mrk 766 can be interpreted physically in the context of an ionised accretion disk in hydrostatic equilibrium [9]. X-ray illumination of the disk leads to the formation of a highly ionised layer at its surface, whose temperature is dependent on the shape of the incident continuum. If the soft flux from the disk is a few times larger than the X-ray illuminating flux, the ionisation equilibrium curves display two main branches, with the upper one consistent with surface layer temperatures of the order of few 100 eV (see Fig. 10, from [4]). Assuming reasonable parameters for the spectral shape of the incident X-ray flux (a power law of photon index 1.8, as measured with *XMM-Newton* in MCG −6-30-15) and of the disk emission (a blackbody of $kT = 10$ eV), and a disk-to-X-ray flux ratio of 6 (a plausible value for AGN), the ionisation equilibrium curve shown in Fig. 10 is expected [4]. Thermal conduction allows only a single ionisation parameter $\Xi_{\rm X}$ (= 1.74 in Fig. 10) at which the transition between hot and cold layers can take place [10]. It can be shown that the fractional abundances of H-like C, N and O along the upper branch are sufficient to explain the equivalent widths observed for the soft X-ray Lyα emission lines of MCG −6-30-15 and Mrk 766, when line transfer effects are taken into account [4]. The real challenge is now to test the applicability of this model to the RGS spectrum of NGC 4051.

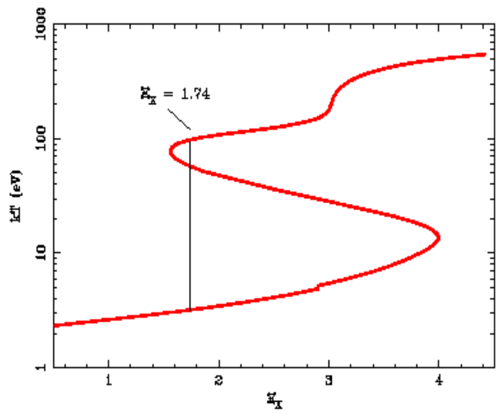

Figure 10. Ionisation equilibrium curve for a power law of photon index 1.8 and a blackbody of temperature $kT = 10$ eV. The vertical line indicates the ionisation parameter $\Xi_{\rm X} = 1.74$ at which the transition from hot to cold phases can take place.

6. Frequency of relativistic lines in AGN

A few other detections of soft X-ray relativistic emission lines have been reported from grating observations, although at lower strength than those found in MCG −6-30-15, Mrk 766 and NGC 4051. One example is that of NGC 4593, where evidence for a N VII line has been reported [11]. The RGS spectrum of NGC 4593 is shown in Fig. 11.

Fig. 12 shows a table listing equivalent widths for the broad soft X-ray O, N and C relativistic emission lines reported to date. They are all from *XMM-Newton* RGS observations, except for those in NGC 5548, which were detected with the *Chandra* LETGS [12]. The table also includes equivalent widths for the broad Fe Kα

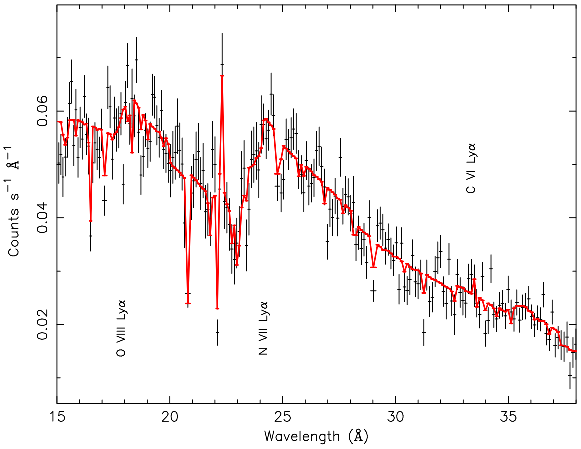

Figure 11. RGS spectrum of NGC 4593; the expected positions of the O VIII, N VII and C VI Lyα emission lines are marked.

lines, derived from *XMM-Newton* EPIC observations. Interestingly, objects with detections of soft X-ray relativistic lines also tend to possess broad Fe lines, and the strengths appear to correlate.

7. Conclusions

A number of Seyfert 1 galaxies have shown evidence for broad soft X-ray spectral features which have been interpreted in terms of relativistically broadened and gravitationally redshifted emission lines; the lines are strong in MCG −6-30-15, Mrk 766 and NGC 4051, but weaker in other objects. Theory shows that they can originate in the hot surface layer of an accretion disk subject to X-ray illumination. It appears that the presence of the soft X-ray features is related to that of a broad Fe Kα line at higher energies, which suggests they may all have a common origin in a relativistic accretion disk surrounding the nuclear black hole.

REFERENCES

1. Branduardi-Raymont, G., Sako, M., Kahn, S. M. et al. 2001, A&A, 365, L140
2. Tanaka, Y., Nandra, K., Fabian, A. C., et al. 1995, Nature, 375, 659
3. Laor, A. 1991, ApJ, 376, 90
4. Sako, M., Kahn, S. M., Branduardi-Raymont, G. et al. 2002, ApJ, submitted (astro-ph/0112436)
5. Sako, M., Kahn, S. M., Behar, E. et al. 2001, A&A, 365, L168
6. Lee, J. C., Ogle, P. M., Canizares, C. R. et al. 2001, ApJL, 554, L13
7. Mason, K. O., Branduardi-Raymont, G., Ogle, P. M., et al. 2003, ApJ, 582, 95
8. Wilms, J., Reynolds, C. S., Begelman, M. C., et al. 2001, Mon. Not. R. Astron. Soc., 328, L27
9. Nayakshin, S. & Kallman, T. R. 2001, ApJ, 546, 406
10. Li, Y. X., Gu, M. F. & Kahn, S. M. 2001, ApJ, 560, 644
11. Steenbrugge, K. C., Kaastra, J. S., Blustin, A. J., et al. 2003, A&A, submitted
12. Kaastra, J. S., Steenbrugge, K. C., Raassen, A. J. J., et al. 2002, A&A, 386, 427
13. Mason, K. O., Branduardi-Raymont, G., Ogle, P. M., et al. 2003, Adv. Space Res., in press
14. Salvi, N. J., Orr, A., Page, M. J., et al. 2003, Mon. Not. R. Astron. Soc., submitted
15. Pounds, K. A., Reeves, J. N., Page, K. L., et al. 2003, Mon. Not. R. Astron. Soc., in press (astro-ph/0210288)
16. Blustin, A. J., Branduardi-Raymont, G., Behar, E., et al. 2002, A&A, 392, 453
17. Blustin, A. J., Branduardi-Raymont, G., Behar, E., et al. 2003, A&A, in press

ACKNOWLEDGEMENTS

This review is based on observations obtained with *XMM-Newton* , an ESA science mission with instruments and contributions directly funded by ESA Member States and the USA (NASA). The MSSL authors acknowledge the support of PPARC. SRON is supported financially by NWO, the Netherlands Organization for Scientific Research.

	Equivalent Width (eV)				
Name	Broad low-energy emission (Grating Spectrometers)			Broad relativistic Fe emission (XMM-EPIC)	Reference
	C	N	O	Fe	
MCG-6-30-15	25	54	162	300-400	1,2,3
Mrk 766	42	96	169	680	1, 4
NGC 4051	-	3:	70	800	5
MCG-2-58-22	-	-	16	135	6
NGC 5548	< 8	22	21	-	7, 8
IRAS 13349+2438	-	-	-		9
NGC 3783	-	-	-	-	10
NGC 7469	-	-	-	-	11
NGC 4593	-	6	-	-	12

Figure 12. Summary of equivalent widths for the soft X-ray relativistic lines and the broad Fe Kα lines of a number of Seyfert galaxies observed with *XMM-Newton* and *Chandra* . References: 1 - [1]; 2 - [4]; 3 - [8]; 4 - [7]; 5 - [13]; 6 - [14]; 7 - [12]; 8 - [15]; 9 - [5]; 10 - [16]; 11 - [17]; 12 - [11]